Hindawi
Advances in Civil Engineering
Volume 2018, Article ID 1387390, 8 pages
https://doi.org/10.1155/2018/1387390

Research Article

Dynamic Compressive Characteristics of Sandstone under Confining Pressure and Radial Gradient Stress with the SHPB Test

Shiming Wang[1,2], **Yunsi Liu**[1,2], **Jian Zhou**[3], **Qiuhong Wu**[4], **Shuyi Ma**[3] and **Zhihua Zhou**[5]

[1]*School of Civil Engineering, Hunan University of Science and Technology, Xiangtan, Hunan 411201, China*
[2]*Hunan Provincial Key Laboratory of Geotechnical Engineering for Stability Control and Health Monitoring, Hunan University of Science and Technology, Xiangtan, Hunan 411201, China*
[3]*School of Resources and Safety Engineering, Central South University, Changsha, Hunan 410083, China*
[4]*Work Safety Key Lab on Prevention and Control of Gas and Roof Disasters for Southern Coal Mines, Hunan University of Science and Technology, Xiangtan, Hunan 411201, China*
[5]*School of Mechanical Engineering, Hunan University of Science and Technology, Xiangtan, Hunan 411201, China*

Correspondence should be addressed to Jian Zhou; csujzhou@hotmail.com

Received 24 April 2018; Revised 28 July 2018; Accepted 10 September 2018; Published 4 November 2018

Guest Editor: Wei Wu

Research on the dynamic compressive characteristics of sandstone under radial gradient stress and confining pressure is conducive to understanding the characteristics of the surrounding rock, especially in an excavation operation for an underground mine roadway and tunnel. The present work aimed at studying the effects of radial gradient stress and confining pressure on the impact of compression of sandstone using a large-diameter split Hopkinson pressure bar. The results showed that the dynamic strength of sandstone under radial gradient stress increased with strain rate following a power function, and the dynamic strength of the sandstone under radial gradient stress was lower and more sensitive to strain rate. The increase in strain at peak stress (peak strain) was linearly correlated with the strain rate under different confining pressures. The sensitivity of the peak strain to confining pressure was lower for the sandstone with a hole, while the values of the elastic modulus were decreased. However, further increasing the stain rate would lead to an increase in the elastic modulus. Also, the ductility of the sandstone with a hole tested in this study was found to improve more significantly. Finally, with an increase in the incident energy, the absorbed energy per unit volume would increase, but would not be affected obviously by the radial gradient stress.

1. Introduction

As a strain-rate sensitive material, the mechanical properties of a rock are affected by dynamic loading and confining pressure and have received a great deal with attention in many engineering fields, particularly excavation-induced seismicity, rockbursts during tunnel excavation and mining activities [1–5]. The dynamic mechanical properties of rock under confining pressure have been widely investigated using many approaches, such as numerical simulations and experimental methods. One commonly used method is a split Hopkinson pressure bar (SHPB), which has been proven as an ideal and a reliable loading technique to measure the dynamic properties of rock at a high strain rate (up to 10^1–10^3 s^{-1}) [6, 7]. Many researchers used Hopkinson bars to study the compressive strength and the dynamic tensile strength of rock-like materials and their rate dependency under uniaxial impact [8–10]. Given the particular requirements, SHPB systems have been significantly improved upon by many researchers [11–13] to obtain a complete triaxial loading test. Thus, the dynamic properties affected by a confining pressure could be better understood using these modified SHPB systems. Both a high loading rate and high confining pressure could increase the compressive

strength of rock material [14–17]. Yin et al. [18] used SHPB to investigate the failure characteristics of rock under static and dynamic loading conditions as well as axial pre-pressure and confining pressure. The results from Yin et al. [18] showed that high-stress rocks under unloading confining pressure were more likely to produce an unstable failure when exposed to the dynamic disturbance. Li et al. [19] proposed a new method for testing the spalling strength at different static preconfining pressures and found that the spalling strength decreased with an increase in the confining pressure. Recently, Guo [20] investigated the dynamic compressive mechanical properties of Beishan granite after high-temperature (25°C to 800°C) treatment under different pressures. In another work, Ma et al. [21] studied the dynamic stress-strain curves for frozen sandy clay which were measured using SHPB and varying the confining pressures (e.g., 0.5, 1.0, and 1.5 MPa) at the freezing temperatures of −5°C and −15°C with strain rates from $160\,s^{-1}$ to $265\,s^{-1}$. The rock was found to be a rate-dependent, temperature-sensitive, and confining pressure-sensitive material. The dynamic peak stress increased with an increase in strain rate and the confining pressure [20, 21]. Tao proposed an experimental method to explore the dynamic failure process of a prestressed rock specimen with a circular hole. Tao obtained the dynamic failure processes and characteristics of a granite specimen with a cavity under different coupled static prestress and dynamic loading experiments conducted on a modified Hopkinson pressure bar system [22, 23]. A significant number of studies have been done to date, but a paucity of research has been devoted to the dynamics of rock materials under confining pressure. For example, in the past, the dynamic mechanical tests of rock under a confining pressure were mainly focused on those measured under equal confining pressure conditions. During excavation for underground structures, such as like tunnels and mine tunnels, the rock surrounding the excavation surface mainly exists in a state of zero normal stress. The hoop stress and the radial stress increase with an increase in radial distance until they achieve the stress of the primary rock [24]. In general, the surrounding rocks of underground mine tunnels exist under radial gradient stress condition, in which they are affected by dynamic loadings such as blasts or machinery during excavation. The stress state of the rock exists under the dynamic loading disturbance, and the radial gradient stress is where the stress increases along the radial gradient stress (see Figure 1). The stress state is different from the static and dynamic mechanisms of the rocks measured under the confining pressure [10]. In this study, a traditional SHPB confining pressure test was done by drilling through the center of the specimen and confining it. According to elastic theory, the stress of the specimen from the center hole to the periphery is a gradient transformation rather than an evenly distributed one, forming a radial gradient stress. The dynamic mechanical properties of the rock under the radial gradient stress were investigated in this study. For comparison, a conventional confining pressure impact test under the same conditions was also performed systematically.

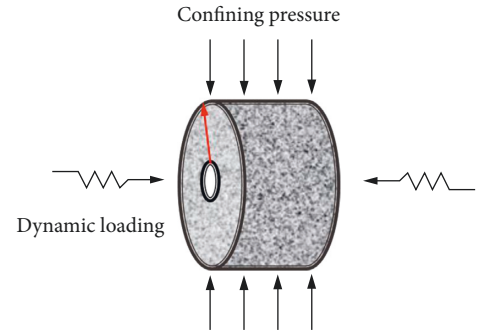

Figure 1: Sketch of the loading state of the rock.

2. Materials and Methods

2.1. Specimen Preparation. According to the requirements for the mechanical test performance of rock, the size of the static load specimen shall be Φ50 mm × 100 mm. Based on the dynamic test principles and existing research results [25], the Φ50 mm × 25 mm was selected as an optimum size for the dynamic load test specimen. According to the requirements for this test, a circular hole with an aperture of 8 mm was drilled along the axis of the specimen in the middle of the cross section (see Figure 2). A 2S-200 vertical coring machine, DQ-4 rock cutting machine, and SHM-200 double-end face grinding machine were used to drill, cut, and polish the rock specimens, to make sure that the surface roughness of the treated specimens was less than 0.02 mm, and the nonparallelism of the upper and lower end faces was less than 0.02 mm. The RMT-150C tester was used to measure the basic mechanical properties of the modified specimens. The static mechanical parameters used in this study are shown in Table 1.

2.2. Test Methods. The impact test was performed on a large-diameter SHPB device (diameter of 50 mm). A flow diagram showing the major steps for the SHPB test is shown in Figure 3 [26]. Hydrostatic confinement was done by connecting two pressure cylinders with two tie rods [7, 11]. The test system was characterized by the medium, and high strain rates for loading were adapted to the heterogeneous brittleness of the rock materials. The strain rate of the obtained specimens ranged from 10^1 to $10^3\,s^{-1}$. A half-sine stress wave was generated on impact using a spindle-type structure punch [27].

To investigate the dynamic mechanical properties of rocks under a radial gradient stress, the major steps employed in the impact test were as follows:

(1) Placing the specimen. The specimen was placed between two long elastic pressure rods, and the end-friction effect was minimized by a smearing butter and installation of the confining pressure device. Since axial pressure was not observed, the two ends were adjusted to clamp the specimen. It should be noted that when the confining pressure was loaded, the specimen was subjected to a certain amount of stress in the axial direction due to Poisson's ratio effect. However, in the ranges of confining pressure and rock strength, its influence would be considered insignificant.

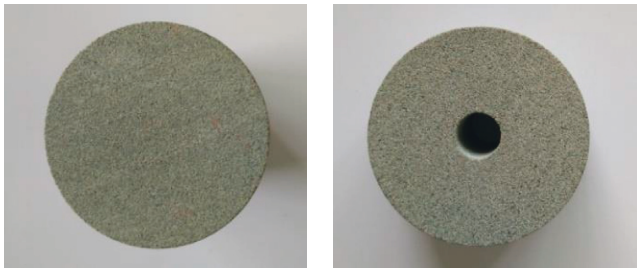

(a) (b)

Figure 2: Specimen: (a) conventional specimen (specimen A) and (b) specimen with a hole (specimen B).

Table 1: Physical-mechanical parameters for sandstone under static load.

Property	Value
Density (kg/m^{-3})	2326
Poisson's ratio	0.196
P-wave speed (m/s)	3185
Compressive strength (MPa)	75.01
Elastic modulus (GPa)	10.18

(2) Loading confining pressures were 5 MPa and 10 MPa in this test.

(3) Adjusting the pressure and taking a single impact. The data acquisition system collected the signal and saved the data until the devices achieved the desired results. Under the same conditions, the impact of the sandstone under conventional confining pressure was also tested. The typical single-impulse waveforms recorded in the test are shown in Figure 4. Parameters such as the stress-strain curve, strain rate, incident energy, transmission energy, and absorption energy of the specimen can be calculated using the following expressions:

$$\sigma = \frac{A_e}{2A_s} E_e \left[\varepsilon_I(t) + \varepsilon_R(t) + \varepsilon_T(t)\right], \quad (1)$$

$$\varepsilon = \frac{C_e}{L_s} \int_0^t \left[\varepsilon_I(t) - \varepsilon_R(t) - \varepsilon_T(t)\right] dt, \quad (2)$$

$$\dot{\varepsilon} = \frac{C_e}{L_s} \left[\varepsilon_I(t) - \varepsilon_R(t) - \varepsilon_T(t)\right], \quad (3)$$

$$E_I = \frac{A_e}{C_e} \int_0^t \varepsilon_I^2(t)\, dt, \quad (4)$$

$$E_R = \frac{A_e}{C_e} \int_0^t \varepsilon_R^2(t)\, dt, \quad (5)$$

$$E_T = \frac{A_e}{C_e} \int_0^t \varepsilon_T^2(t)\, dt, \quad (6)$$

$$E_s = E_I - E_R - E_T, \quad (7)$$

where $A_e$is the elastic rod area, $A_s$is the area of the specimen, $\rho_e$is the elastic rod density, C_e is the velocity of the elastic rod, $L_s$is the length of the specimen, t is the duration of the stress wave, $E_s$is the absorption energy of the specimen, and E_I, E_R, and E_T are the incident, reflected, and transmitted energies, respectively.

It should be noted that, due to exist of the confining pressure, the specimen was not prone to crack or break. All of the specimens in the impacted experiments tested were not obviously cracked or broken and just presented with slight cracks. The effects of the gradient stress on the stress-strain curve, strength, deformation, and energy absorption characteristics of the specimen were investigated without obvious failure in this study.

3. Results

Figure 4 shows the impact waveforms for the two test specimens. From the figure, it can be seen that the waveforms of the specimen (denoted as specimen B) under radial gradient stress had a larger reflected wave and a smaller transmitted wave than those of the specimen (denoted as specimen A) under radial uniform stress. When combined with stress wave theory and Equations (1) and (3), it shows that at the same level of impact, specimen B had a lower strength and a higher strain rate.

Figure 5 shows the dynamic stress-strain curves for sandstone impacted under different radial stresses. It shows that their curve shapes are similar. In comparison with specimens under radial uniform stress, the stress-strain curve of the sandstone under radial gradient stress was slower, and lower elastic modulus, lower strength, and higher peak strain were found, especially in the initial stage and in the postpeak stage. The above phenomenon could be found to be more significant as the level of impact increases, whereas it would be reduced with an increase in the confining pressure. It can be seen from Figure 5 that the strength decreased but the peak strain was much larger when the level of impact increases or decreases with an increase in the confining pressure. The differences between Figures 4 and 5 suggest that the transflective capacity of the stress waves and stress-strain curve are more moderate for the specimen with a hole, and the dynamic mechanical properties of the sandstone under radial gradient stress were different from those occurring under conventional confining pressure conditions.

3.1. Strength. Rock is a strain rate sensitive material, and both the tensile strength and compressive strength increase with increasing strain rate [10, 14–17]. Figure 6 shows the variation in the dynamic strength of sandstone with strain rate under different confining pressures. It can be seen that under different radial stress states, the dynamic strength undergoes an exponential increase with an increase in the strain rate, and it was also found that under higher confining pressures, the dynamic strength was increased more significantly. This finding was consistent with most previous re-

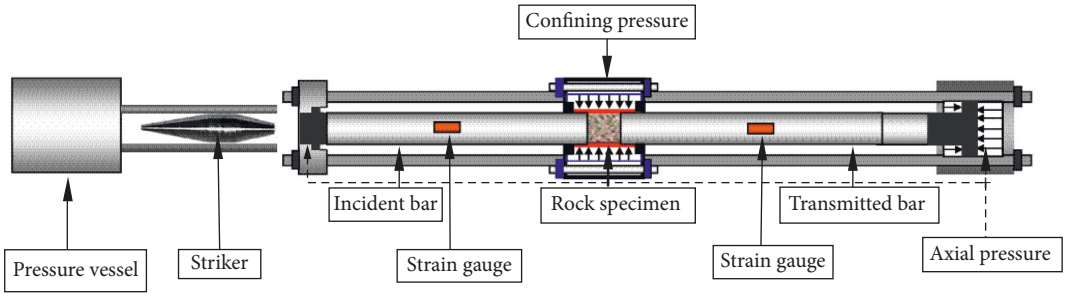

Figure 3: A flow diagram of SHPB (the experimental system).

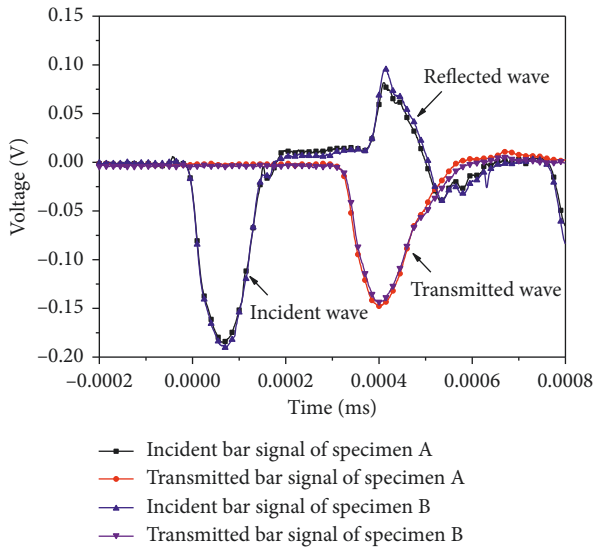

Figure 4: Typical waveform of a compression test.

search [11–13]. The data in the red circle in Figure 6 are the dynamic strength at the same impact level under different confining pressure conditions. Figure 6 shows that under the same impact level, the dynamic strength under radial gradient stress was smaller than under radial uniform stress, and the corresponding strain rate was relatively higher. This result was similar to those occurring under static loading conditions [28]. As seen from the fitting functions shown in Figure 6, although the strength of the specimen under radial gradient stress was lower, it was more sensitive to the strain rate than the specimen under radial uniform stress under two levels of confining pressure. The phenomenon becomes more apparent with increases in the confining pressure. The findings implied that the dynamic strength of the sandstone under radial gradient stress was more sensitive to the strain rate and the confining pressure. Therefore, the dynamic strength of the rock under gradient stress would be different from those of the specimens under conventional confining pressure conditions.

3.2. Deformation. Figure 7 shows the variation in peak strain with strain rate under different radial stress conditions. The peak strain had a linearly increase in the strain rate under different confining pressures [29]. As shown in Figure 7, the growth rate of the peak strain decreased with the increase in strain rate and the confining pressure under radial gradient stress conditions. It was sensitive to the increased confining pressure under radial uniform stress. The sensitive of peak strain to the strain rate for the specimen with a hole is smaller compared with that of intact specimen under two levels of confining pressure conditions. A possible explanation for the change in sensitivity would be that the exit of the hole provides a free surface for the specimen with a hole and allows the specimen to have better deformability. It is less sensitive to strain rate, and with the increase in the confining pressure, the deformability caused by the free surface had become smaller. The deformability for the specimen with a hole is improved. The red circle in the figure shows the peak strain of sandstone at the same level of impact. The findings showed that the peak strain of the sandstone under radial gradient stress was greater than under radial uniform stress, but the difference between them would decrease with an increase in the confining pressure. These results implied that the deformation capability of the rock under radial gradient stress was enhanced, which could be proven using the results in Figure 5. The main reason for the higher strain rate in the rock under radial gradient stress at the same level of impact was possibly attributed to a good capability for deformation.

Since the stress-strain curve under dynamic loading was not a straight line, we analyzed the secant modulus (E_{50}). Figure 8 shows the changes in E_{50} with strain rate. It can be seen from the figure that the dynamic E_{50} of the sandstone under different radial stress conditions showed two modes with the increase of the strain rate. Although the E_{50} of the rock under the radial uniform stress increased with the increase in strain rate, the change was not obvious and was consistent with the findings reported by Gong [30]. The E_{50} of rock under a radial gradient stress decreased first and then increased with an increase in the strain rate. The phenomenon was mainly due to that the exit of the hole provides greater deformability for the specimen with a hole compared with the intact specimen. And the E_{50} of the rock under the radial uniform stress would decrease. Due to the small size of the hole, the deformability provided by the free faces of the hole is limited. With the increase of strain rate, the E_{50} would increase, but the change was also not obvious. What is more, the difference in sensitivity between the dynamic strength and peak strain at the strain rate may have an influence on the E_{50} increased with the strain rate. From Figure 8, it can be seen

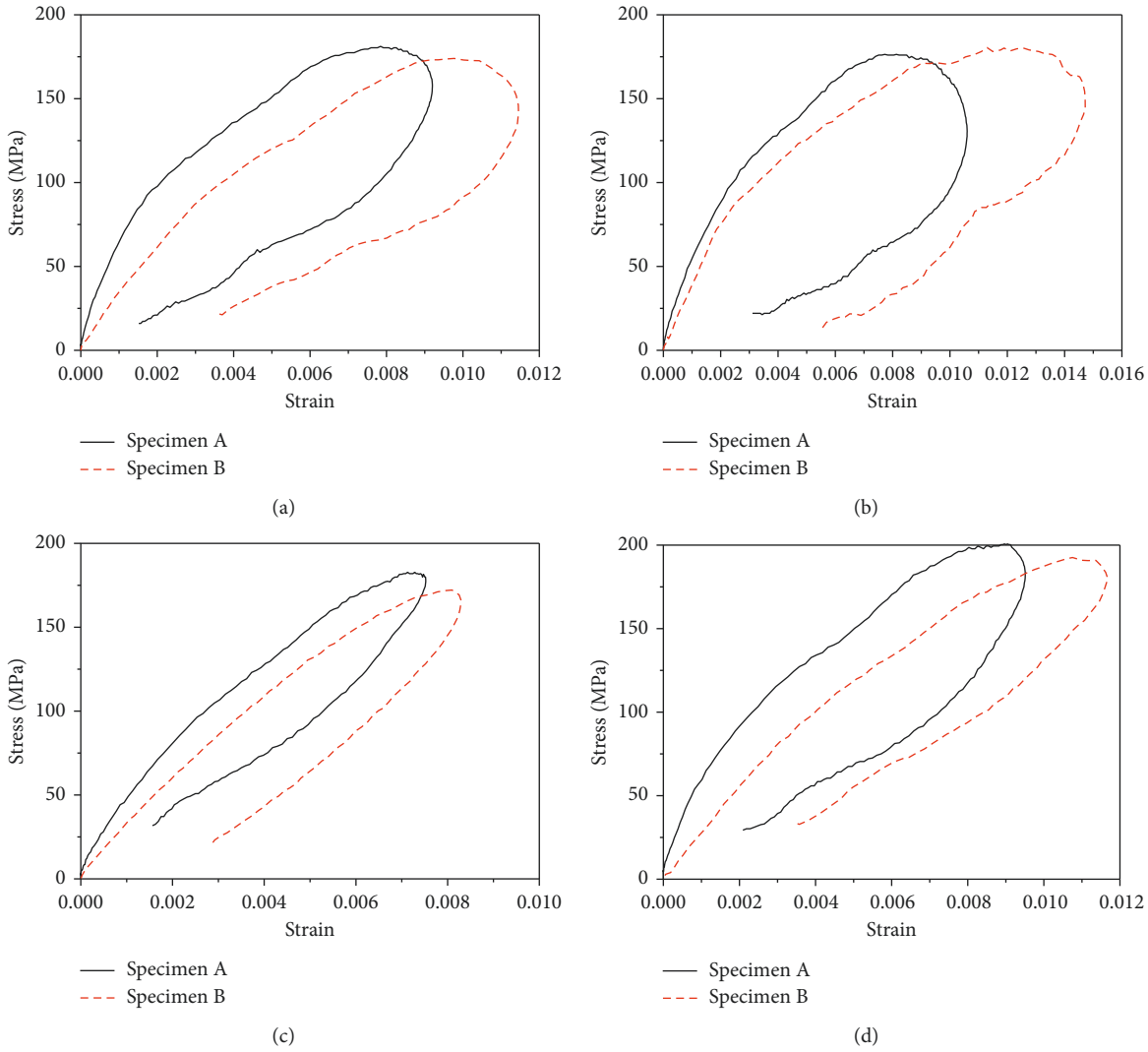

Figure 5: Stress and strain curves for the sandstone under dynamic loading with (a) impact at 0.6 MPa pressure under a confining pressure of 5 MPa, (b) impact at 0.7 MPa pressure under a confining pressure of 5 MPa, (c) impact at 0.6 MPa pressure under a confining pressure of 10 MPa, and (d) impact at 0.7 MPa pressure under a confining pressure of 10 MPa.

that the E_{50} of the sandstone under a radial gradient stress showed a discrete in comparison with that of the sandstone under radial uniform stress. That may be due to the drilling process for the specimen which will inevitably affect the mechanical properties of the specimen. The data in red circle are the E_{50} of the sandstone that was impacted at the same level under different confining pressure conditions. The E_{50} of the sandstone under radial gradient stress was far less than that under radial uniform stress. When combined with the results in Figures 7 and 8, it could be concluded that the ductility of the sandstone under radial gradient stress was improved.

3.3. Energy Absorption. Figure 9 shows the energy absorption properties of sandstone under different confining pressure conditions. As seen in Figure 9, the absorption energy per unit volume of sandstone increased with an increase in incident energy. The change in absorption energy of most rock-like materials also followed the above trend [31, 32]. The magnitude increase would be reduced with an increase in confining pressure in this study, regardless of whether the specimen was under radial uniform stress or under radial gradient stress. The relationship between the absorption energy per unit volume and the incident energy was not significantly affected by the radial gradient stress. That is mainly because the specimens were not obviously cracked or broken and just presented with a slight crack, and the absorbed energy is mainly consumed by the expansion and formation of microcracks.

4. Discussion

Due to the existence of a hole, specimen B has a free surface, which will allow the specimen to have greater deformability. The initial stress of the specimen is radial gradient stress and implies that the holes had a greater influence on the mechanical properties of the specimen according to previous research [29, 33–35]. The holes allowed a greater deformation

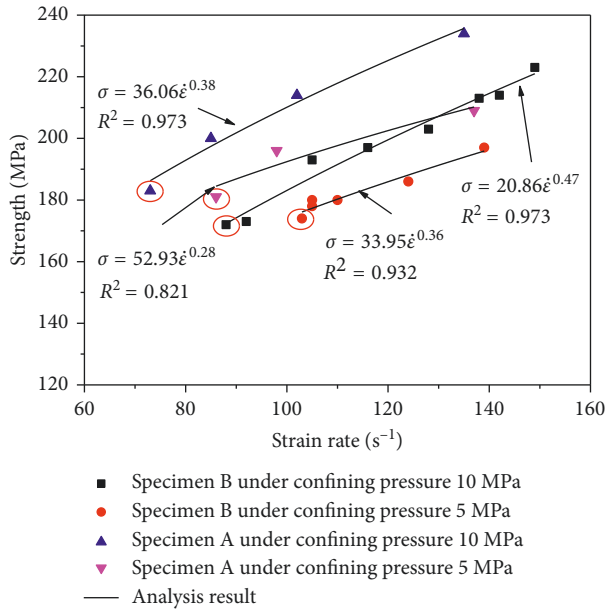

Figure 6: Variation in dynamic strength with strain rate.

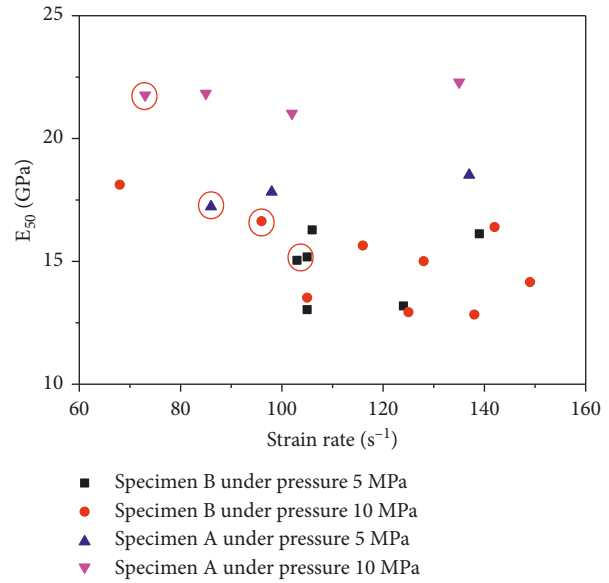

Figure 8: Variation in E_{50} with strain rate.

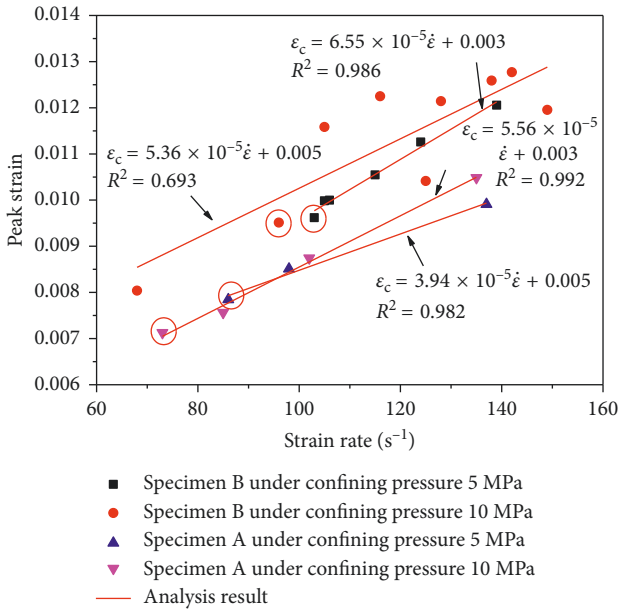

Figure 7: Variation in peak strain with strain rate.

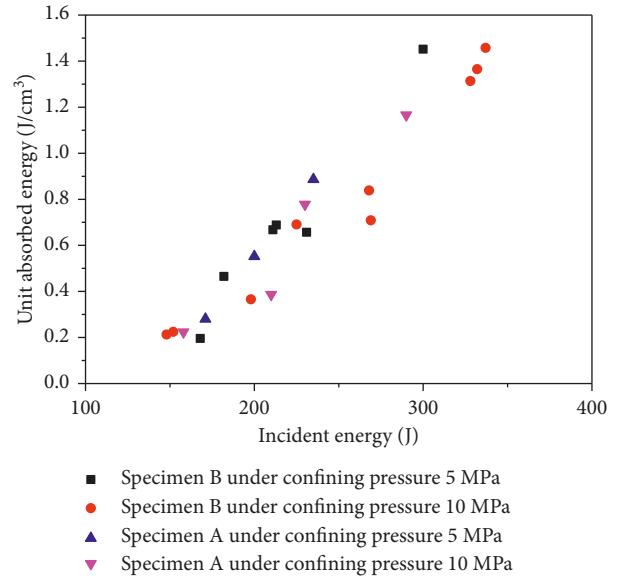

Figure 9: Variation in absorbed energy per unit volume with incident energy.

of the specimen in the radial direction. The confining pressure effect was also smaller and resulted in a higher strain rate and a lower strength of the sandstone under radial gradient stress at the same impact level. More importantly, the dynamic strength of the sandstone under radial gradient stress was more sensitive to the strain rate. Many researchers have observed that at higher rates of loading, stronger concretes exhibit a smaller percentage gain in compressive strength than weaker concretes [36]. Cowell suggested that the improvement noted for weak concretes may be influenced more by their lower static strength when expressed as a proportion of this smaller value [37]. The hole diameter has no effect on the uniaxial compressive strength of hollow sandstone when the hole diameter is smaller than 10 mm [28, 29]. This means that the difference in strain rate sensitivity was not due to static strength differences. Hence, the sensitivity of the strain rate for the sandstone with a hole may be improved due to greater deformability and radial gradient stress and needs to be investigated through further research. Although the exit of the hole provides greater deformability for the specimen with a hole compared with the intact specimen, due to the small size of the hole, the deformability provided by the free faces of the hole is limited. What is more, the difference in sensitivity between dynamic strength and peak strain at a particular strain rate may have an influence on the E_{50} increased with the

strain rate. Both of them would result in the E_{50} of rock under radial gradient stress showing a trend that decrease first and then increase with the increase in the strain rate. The above findings provide guidance for improvement on practical engineering projects, such as tunnels and roadways, since the surrounding rock is in similar gradient stress conditions.

In this study, only the dynamic compressive characteristics of sandstone were investigated at two levels of confining pressure. The failure modes under different confining pressures and stress distributions for different specimens were not examined. The hole size effect was also not investigated. Therefore, many other types of rocks of interest should be investigated using the aforementioned methodology in the future.

5. Conclusions

In this study, impact compression tests of sandstone under different confining pressures were conducted with SHPB. The effect of the mechanical properties of the specimens under radial gradient stress was compared with those under radial uniform stress. The conclusions we obtained in this study are as follows:

(1) The dynamic strength and the strain rate of sandstone had an exponential increase. The dynamic strength of the rock under radial gradient stress was smaller than that occurring under radial uniform stress, but the former was more sensitive to strain rate.

(2) The increase in peak strain was linearly correlated with the strain rate under different confining pressures, while the sensitivity of the peak strain to confining pressure was lower for the sandstone with a hole. The values of the E_{50} were decreased, but further increasing the stain rate would lead to an increase in the level of the elastic modulus, which is different than under radial uniform stress. Also, the ductility of the sandstone under radial gradient stress could be improved.

(3) Although the absorption energy per unit volume of sandstone increased with an increase in incident energy and its growth rate was decreased with the increase in the confining pressure, the relationship between the absorption energy per unit volume and the incident energy was not significantly affected by the radial gradient stress.

Data Availability

No data were used to support this study.

Conflicts of Interest

The authors declare that they have no conflicts of interest.

Acknowledgments

This work was supported by financial grants from the National Natural Science Foundation of China (51604109, 51704109, 51504092, 51509242, and 41807259), the Natural Science Foundation of Hunan Province (2018JJ3693), the China Postdoctoral Science Foundation funded project (2017M622610), and the Foundation of Hunan Educational Committee (16C0646). The authors acknowledge financial contribution and appreciate the organizations that supported this basic research.

References

[1] W. Wu, Z. Zhao, and K. Duan, "Unloading-induced instability of a simulated granular fault and implications for excavation-induced seismicity," *Tunnelling & Underground Space Technology*, vol. 63, pp. 154–161, 2017.

[2] Y. Li, W. Wu, and B. Li, "An analytical model for two-order asperity degradation of rock joints under constant normal stiffness conditions," *Rock Mechanics & Rock Engineering*, no. 1, pp. 1–15, 2018.

[3] X. Li, J. Zhou, S. Wang, and B. Liu, "Review and practice of deep mining for solid mineral resources," *Chin J Nonferrous Metals*, vol. 27, no. 7, pp. 1236–1262, 2017.

[4] J. Zhou, X. Li, and H. S. Mitri, "Classification of rockburst in underground projects: Comparison of ten supervised learning methods," *Journal of Computing in Civil Engineering*, vol. 30, no. 5, article 04016003, 2016.

[5] M. Wang, X. Shi, J. Zhou, and X. Qiu, "Multi-planar detection optimization algorithm for the interval charging structure of large-diameter longhole blasting design based on rock fragmentation aspects," *Engineering Optimization*, vol. 50, no. 12, pp. 2177–2191, 2018.

[6] H. Kolsky, "An investigation of the mechanical properties of materials at very high rates of loading," *Proceedings of the Physical Society B*, vol. 62, no. 11, pp. 676–700, 1949.

[7] K. Xia and W. Yao, "Dynamic rock tests using split Hopkinson (Kolsky) bar system—A review," *Journal of Rock Mechanics and Geotechnical Engineering*, vol. 7, no. 1, pp. 27–59, 2015.

[8] Q. M. Li, Y. B. Lu, and H. Meng, "Further investigation on the dynamic compressive strength enhancement of concrete-like materials based on split Hopkinson pressure bar tests. Part II: numerical simulations," *International Journal of Impact Engineering*, vol. 36, no. 12, pp. 1327–1334, 2009.

[9] Y. B. Lu and Q. M. Li, "About the dynamic uniaxial tensile strength of concrete-like materials," *International Journal of Impact Engineering*, vol. 38, no. 4, pp. 171–180, 2011.

[10] F. Q. Gong and G. F. Zhao, "Dynamic indirect tensile strength of sandstone under different loading rates," *Rock Mechanics & Rock Engineering*, vol. 47, no. 6, pp. 2271–2278, 2014.

[11] X. B. Li, Z. L. Zhou, T. S. Lok, L. Hong, and T. B. Yin, "Innovative testing technique of rock subjected to coupled static and dynamic loads," *International Journal of Rock Mechanics and Mining Sciences*, vol. 45, no. 5, pp. 739–748, 2008.

[12] D. J. Frew, S. A. Akers, W. Chen, and M. L. Green, "Development of a dynamic triaxial Kolsky bar," *Measurement Science and Technology*, vol. 21, no. 10, pp. 1057–1060, 2010.

[13] P Bailly, F Delvare, J Vial et al., "Dynamic behavior of an aggregate material at simultaneous high pressure and strain rate: SHPB triaxial tests," *International Journal of Impact Engineering*, vol. 38, no. 2-3, pp. 73–84, 2011.

[14] M. Hokka, J. Black, D. Tkalich et al., "Effects of strain rate and confining pressure on the compressive behavior of Kuru

granite," *International Journal of Impacting Engineering*, vol. 91, pp. 183–193, 2016.

[15] H. Yang, H. Song, and S. Zhang, "Experimental investigation of the behavior of aramid fiber reinforced polymer confined concrete subjected to high strain-rate compression," *Construction & Building Materials*, vol. 95, pp. 143–151, 2015.

[16] C. Qi, M. Wang, J. Bai, and K. Li, "Mechanism underlying dynamic size effect on rock mass strength," *International Journal of Impacting Engineering*, vol. 68, pp. 1–7, 2014.

[17] Q. B. Zhang and J. Zhao, "A review of dynamic experimental techniques and mechanical behaviour of rock materials," *Rock Mechanics & Rock Engineering*, vol. 47, no. 4, pp. 1411–1478, 2014.

[18] Z. Q. Yin, X. B. Li, J. F. Jin et al., "Failure characteristics of high stress rock induced by impact disturbance under confining pressure unloading," *Transactions of Nonferrous Metals Society of China*, vol. 22, no. 1, pp. 175–184, 2012.

[19] X. B. Li, M. Tao, C. Wu et al., "Spalling strength of rock under different static pre-confining pressures," *International Journal of Impact Engineering*, vol. 99, pp. 69–74, 2017.

[20] H. Guo, W. Guo, Y. Zhai et al., "Experimental and modeling investigation on the dynamic response of granite after high-temperature treatment under different pressures," *Construction & Building Materials*, vol. 155, pp. 427–440, 2017.

[21] D. D. Ma, Q. Y. Ma, and P. Yuan, "SHPB tests and dynamic constitutive model of artificial frozen sandy clay under confining pressure and temperature state," *Cold Regions Science and Technology*, vol. 136, pp. 37–43, 2017.

[22] M. Tao, A. Ma, W. Z. Cao, X. B. Li, and F. Q. Gong, "Dynamic response of pre-stressed rock with a circular cavity subject to transient loading," *International Journal of Rock Mechanics and Mining Sciences*, vol. 99, pp. 1–8, 2017.

[23] M. Tao, H. T. Zhao, X. B. Li, X. Li, and K. Du, "Failure characteristics and stress distribution of pre-stressed rock specimen with circular cavity subjected to dynamic loading," *Tunnelling and Underground Space Technology*, vol. 81, pp. 1–15, 2018.

[24] B. H. G. Brady and E T. Brown, *Rock Mechanics for Underground Mining*, Allen & Unwin, Crows Nest, Australia, 2006.

[25] Y. X. Zhou, K. Xia, X. B. Li et al., "Suggested methods for determining the dynamic strength parameters and mode-I fracture toughness of rock materials," *International Journal of Rock Mechanics & Mining Sciences*, vol. 49, no. 1, pp. 105–112, 2012.

[26] F. Q. Gong, X. B Li, and X. L. Liu, "Preliminary experimental study of characteristics of rock subjected to 3D coupled static and dynamic loads," *Chinese Journal of Rock Mechanics and Engineer*, vol. 30, no. 6, pp. 1179–1190, 2011.

[27] X. B. Li, T. S. Lok, J. Zhao et al., "Oscillation elimination in the Hopkinson bar apparatus and resultant complete dynamic stress-strain curves for rocks," *International Journal of Rock Mechanics and Mining Sciences*, vol. 37, no. 7, pp. 1055–1060, 2000.

[28] M. You and C. Su, "Study of strength and failure of hollow cylinders and rings of sandstone under compression-tension stress," *Chinese Journal of Rock Mechanics and Engineering*, vol. 29, no. 6, pp. 1096–1105, 2010.

[29] S. Q. Yang, "Experimental study on deformation, peak strength and crack damage behavior of hollow sandstone under conventional triaxial compression," *Engineering Geology*, vol. 213, pp. 11–24, 2016.

[30] F. Gong, *Experimental Study of Rock Mechanical Properties Under Coupled Static-Dynamic Loads and Dynamic Strength Criterion*, Central South University, Changsha Shi, China, 2010.

[31] X. Li, S. Wang, L. Weng, L. Huang, T. Zhou, and J. Zhou, "Damage constitutive model of different age concrete under impact load," *Journal of Central South University*, vol. 22, no. 2, pp. 693–700, 2015.

[32] S. Wang, L. Dong, and J. Zhou, "Influence of early age on the wave velocity and dynamic compressive strength of concrete based on split Hopkinson pressure bar tests," *Shock and Vibration*, Article ID 8206287, 8 pages, 2018.

[33] Y. Zhao, L. Zhang, W. Wang, W. Wan, and W. Ma, "Separation of elastoviscoplastic strains of rock and a nonlinear creep model," *International Journal of Geomechanics*, vol. 18, no. 1, Article 04017129, 2018.

[34] Y. Zhao, Y. Wang, W. Wang et al., "Modeling of non-linear rheological behavior of hard rock using triaxial rheological experiment," *International Journal of Rock Mechanics & Mining Sciences*, vol. 93, pp. 66–75, 2017.

[35] Y. Zhao, L. Zhang, W. Wang et al., "Transient pulse test and morphological analysis of single rock fractures," *International Journal of Rock Mechanics & Mining Sciences*, vol. 91, pp. 139–154, 2017.

[36] P. H. Bischoff and S. H. Perry, "Compressive behaviour of concrete at high strain rates," *Materials & Structures*, vol. 24, no. 6, pp. 425–450, 1991.

[37] W. L. Cowell, "Dynamic properties of plain Portland cement concrete," *Dynamic Properties of Plain Portland Cement Concrete*, 1966.